

REGISTRATION-BASED RANGE-DEPENDENCE COMPENSATION METHOD FOR CONFORMAL-ARRAY STAP

Xavier Neyt*, Philippe Ries†, Jacques G. Verly†, Fabian D. Lapierre*

*Royal Military Academy, Department of Electrical Engineering,
Avenue de la Renaissance, 30, B-1000, Bruxelles, Belgium

{Xavier.Neyt, Fabian.Lapierre}@elec.rma.ac.be

†University of Liège, Department of Electrical Engineering and Computer Science,
Sart-Tilman, Building B28, B-4000 Liège, Belgium

Jacques.Verly@ulg.ac.be, ries@montefiore.ulg.ac.be

ABSTRACT

We first generalize the concept of clutter power spectrum locus so that it can be applied to arbitrary antenna arrays. This locus is a curve in the 4D space of the Doppler frequency and the 3 spatial frequencies. This generalization is valid for both monostatic and bistatic radar configurations. We show that the customary clutter power spectrum locus representation in the 2D space of the Doppler frequency and the single spatial frequency used when considering linear arrays is a projection of the 4D curve. This projection property furthermore provides a very simple interpretation of the evolution of the 2D clutter power spectrum locus in function of the crab angle (angle between the antenna reference direction and the platform velocity vector).

We then extend the registration-based clutter range-dependence compensation method developed in [1, 2] to arbitrary antenna arrays. Finally, we evaluate the performance in terms of SINR loss and show that this method can achieve near-optimum detection performance.

1. INTRODUCTION

In downlooking airborne radars, echoes from slow-moving targets compete with clutter returns. Detecting these targets can be done using space-time adaptive processing (STAP). This involves computing the optimum filter that filters as best as possible the interferences (and the noise) out of the received signal. Computing this filter requires an estimate of the interference + noise covariance matrix (CM) at the range of interest. This CM is commonly computed by averaging single-realization sample CM at neighboring ranges. However, this estimation method requires that the contributing data snapshots be independent and identically distributed (IID). Range-varying clutter returns, e.g., due to geometry-

induced non-stationarity, affect the accuracy of the estimated CM.

When a monostatic sidelooking linear array geometry is considered, the snapshots at different ranges are typically identically distributed [3, 4]. However, most bistatic and non sidelooking configurations lead to a geometry-induced range-dependent clutter-signal CM [1, 5] even with a linear array.

Non-linear arrays (i.e., with elements that may not all be along a straight line) and, in particular, conformal arrays offer major practical advantages over linear arrays. Indeed, conformal arrays adopt the shape of the carrier thus maintaining its aerodynamic characteristics. This in turn allows to build larger arrays, thus providing a higher spatial resolution leading to a smaller minimum detectable velocity. However, non-linear arrays induce a range-dependent clutter in most monostatic and bistatic configurations. Designing STAP algorithms for non-linear arrays is thus challenging. STAP applied to circular arrays is considered in [6, 7] while [8, 9, 10] consider conformal arrays.

The remainder of the paper is organized in the following manner. In Section 2, the concept of 2D clutter power spectrum (PS) locus for linear arrays is reviewed and subsequently generalized to 4D for non-linear arrays. The relationship between the clutter PS locus and the clutter PS is then deduced. Section 3 discusses the range-dependence of the clutter statistics. In Section 4, the range-dependence compensation method presented in [1, 2] is reviewed and generalized to non-linear arrays. Finally, Section 5 presents the performance of the proposed range-dependence compensation method in terms of SINR loss and compares it to that of the optimum processor.

2. 4D CLUTTER POWER SPECTRUM

2.1. Power spectrum locus

We first consider a continuous space-time random signal field $x(\mathbf{r}, t)$ with zero mean. This signal is defined in the 4D space of the 3 spatial coordinates $\mathbf{r} = (x, y, z)$ and the time t . Assuming the signal is wide-sense stationary in space and in time, its covariance function takes the form

$$\rho(\Delta\mathbf{r}, \Delta t) = E\{x(\mathbf{r}, t)x^*(\mathbf{r} - \Delta\mathbf{r}, t - \Delta t)\}. \quad (1)$$

The 4D PS of the signal $x(\mathbf{r}, t)$ is defined as the Fourier transform (FT) of its covariance [11, 12]

$$P(\mathbf{k}, \omega) = \iiint_{-\infty}^{\infty} \iiint_{-\infty}^{\infty} \rho(\Delta\mathbf{r}, \Delta t) e^{-j(\mathbf{k} \cdot \Delta\mathbf{r} + \omega \Delta t)} d\Delta\mathbf{r} d\Delta t, \quad (2)$$

where $\mathbf{k} = (k_x, k_y, k_z)$. This PS can be interpreted as representing the energy of the plane waves with temporal frequency ω and arriving from direction \mathbf{k} [11, 12].

We now consider the signal components due to the clutter. The clutter is modeled as the superposition of a large number of independent clutter sources [3, 9] located along the isorange of interest. Range ambiguities are neglected. Each clutter patch contributes a signal corresponding to a distinct direction of arrival \mathbf{k} . Hence, the signal from each clutter patch will correspond to a distinct point in the spatio-temporal frequency domain (\mathbf{k}, ω) . This can be thought of as if the isorange in the 3D spatial domain was imaged into another curve in the 4D frequency domain (\mathbf{k}, ω) . For this reason, we will call this 4-dimensional curve in the frequency domain the *4D clutter power spectrum (PS) locus*. Notice that this curve is independent of the characteristics of the antenna. Figure 1 illustrates the 4D clutter PS locus. The representation consists of two graphs¹. The first graph is a projection in the 3D space (k_x, k_y, ω) , while the second graph is a projection in the 3D space (k_x, k_y, k_z) of the spatial frequencies. Since the norm of \mathbf{k} is constant, the latter representation of the projection of the 4D clutter PS locus yields a curve on a (3D) sphere.

The correlation function

$$\rho(\Delta\mathbf{r}, \Delta t) = \rho(\Delta x, \Delta y, \Delta z, \Delta t) \quad (3)$$

corresponds to all possible vector lags $\Delta x, \Delta y$ and Δz in 3D (x, y, z) space. To measure such lags, we need a 3D antenna. (At this point, we do not worry about sampling $x(\mathbf{r}, t)$: we imagine that we can measure ρ for all possible 3D spatial lags.) Now imagine that we can only measure the

¹The coordinate system in the graphs was normalized. The relation between the normalized spatial frequency vector $\nu_s = (\nu_{sa}, \nu_{sc}, \nu_{sv})$ and the wavenumber vector \mathbf{k} is $\nu_s = \mathbf{k} \frac{\lambda}{2\pi} \frac{1}{2}$, where λ is the wavelength at the carrier frequency. The relation between the normalized Doppler frequency ν_d and the Doppler pulsation ω is $\nu_d = \omega \frac{PRI}{2\pi}$, where PRI is the pulse repetition interval.

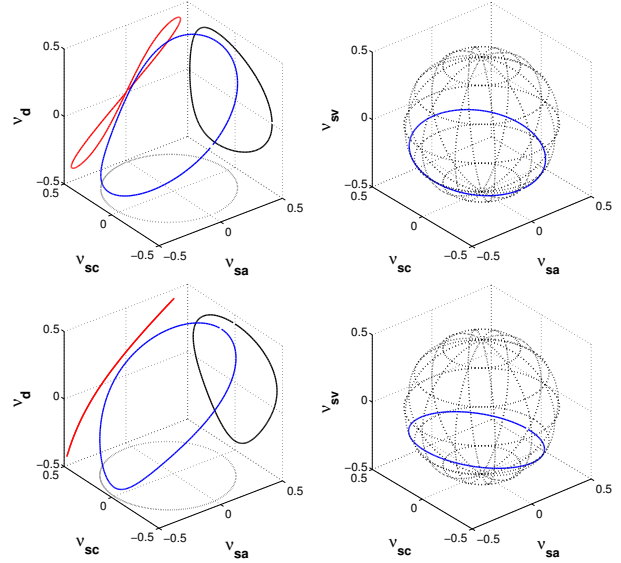


Figure 1: 4D clutter power spectrum locus: wing-to-wing formation (upper row); in-trail formation (lower row).

vector lags $(\Delta x, 0, 0)$, i.e., those aligned with the x -axis. (once again, we don't worry about sampling.) Then, instead of being able to "measure" $\rho(\Delta\mathbf{r}, \Delta t)$, we can now only measure $\rho(\Delta x, \Delta t)$. Let us denote the 2D FT of $\rho(\Delta x, \Delta t)$ by $P_l(k_x, \omega)$. Of course, $P_l(k_x, \omega)$ is nothing, but the 2D PS commonly encountered in STAP for a continuous linear antenna. It is thus legitimate to ask whether there is a relation between the 2D function $P_l(k_x, \omega)$ and the 4D function $P(\mathbf{k}, \omega)$. The answer lies in a generalization to 4D of the conventional 2D projection-slice theorem of computerized tomography [13] (with the domains reversed). Indeed, the generalized theorem tells us that $P_l(k_x, \omega)$ is simply the integral of $P(\mathbf{k}, \omega)$ along the planes parallel to the plane $k_y = k_z = 0$ and going through each (k_x, ω) , i.e.,

$$P_l(k_x, \omega) = \frac{1}{4\pi^2} \iint P(k_x, k_y, k_z, \omega) dk_y dk_z. \quad (4)$$

Whereas this relation can easily be proven from first principles, the power of the theorem lies in the fact that it also applies to any orientation of the linear antenna in space.

In the case of a linear antenna, we know that a real 2D clutter PS exhibits a so-called clutter ridge and that in the limit for an infinitely long antenna and for a continuous wave, the 2D PS is concentrated on a 2D curve. This curve which can also be obtained by physical reasoning, is called angle-Doppler curve, direction-Doppler (DD) curve or (2D) clutter PS locus [1, 3, 9, 14]. This curve is also called the clutter ridge by abuse of language. The shape of this 2D clutter PS locus varies in a complex way with changes in the geometric configuration [1, 5, 15]. Examples are shown in Fig. 2. The notion of 2D clutter PS locus immediately

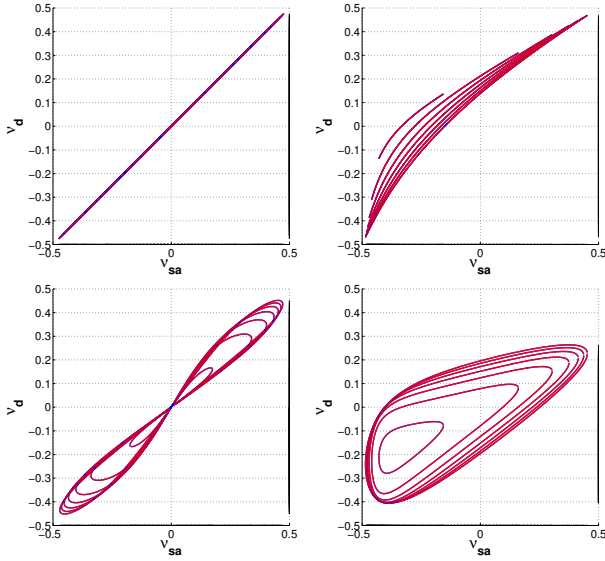


Figure 2: 2D clutter power spectrum locus for different geometries and at different ranges.

extends to 4D.

$P_l(k_x, \omega)$ (a function) being the projection of $P(\mathbf{k}, \omega)$, it immediately follows that the 2D clutter PS locus (a curve) is the projection of the 4D clutter PS locus. In other words, once we know the 4D clutter PS locus in (\mathbf{k}, ω) space, we can immediately obtain its 2D counterpart in any 2D plane, e.g., that corresponding to (k_x, ω) , which is the customary 2D clutter PS locus. Therefore, many of the complex behavior can now be understood in terms of the projection of the 4D clutter PS locus on a 2D plane.

For example, the effect of a non-zero crab angle (angle between k_x and the velocity vector assumed horizontal) on the 2D clutter PS locus is difficult to interpret, while it simply results in a rotation of the 4D clutter PS locus around the k_z axis as illustrated in Fig. 3.

2.2. Sampling

In real radar systems, only samples $x(\mathbf{r}_n, t_m)$ of the signal field $x(\mathbf{r}, t)$ are available. The temporal samples t_m correspond to the time at which the pulses are emitted. For a constant PRI, one has $t_m = mPRI$. The spatial sampling correspond to the actual location of the array elements. For a uniform linear array (ULA) aligned with the x -axis, one has $\mathbf{r}_n = nd\mathbf{1}_x$ where d is the distance between two adjacent antenna elements and $\mathbf{1}_x$ is a unit vector aligned with the x -axis. The set of $N \times M$ samples of a particular range gate, measured at the N antenna elements resulting from the M pulses is called a snapshot and usually put in the form of a lexicographically-ordered vector \mathbf{x} .

The covariance matrix \mathbf{R} of the random vector \mathbf{x} can be computed. It should be noted that the covariance matrix will

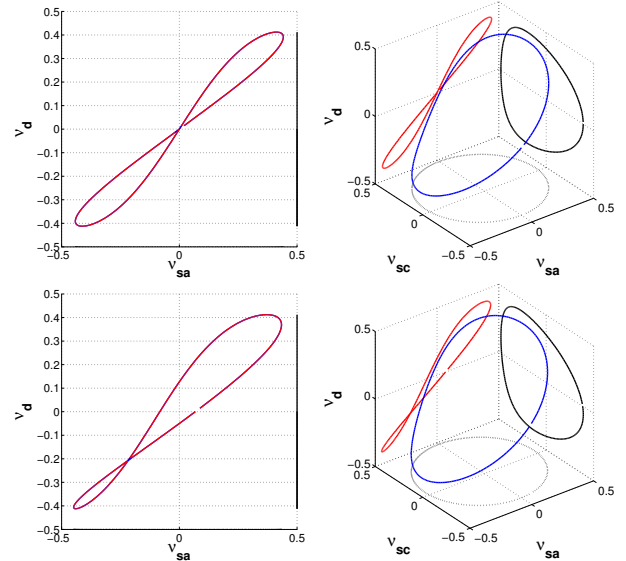


Figure 3: 2D and 4D clutter power spectrum locus². The graphs in the upper row are drawn for a scenario with a crab-angle of 0° while the graphs of the lower row are drawn for the same scenario, but with a crab-angle of 10° .

exhibit the usual Toeplitz-block-Toeplitz structure only if a ULA and a constant PRI are considered.

The PS of the signal x can be estimated from the covariance matrix of \mathbf{x} using, e.g., the Fourier transform or the minimum variance estimator (MVE) [11, 12]. If the clairvoyant covariance matrix is used, the estimation error will only be due to the fact that a finite number of samples was available to perform the PS estimation. An additional source of estimation error occurs if an estimate of the covariance matrix is used instead of the clairvoyant one. To simplify the discussion, we will consider that the clairvoyant covariance matrix is used in the remainder of this section.

In [12] and in the case of the two spectral estimator mentioned in the previous paragraph, it is shown that the estimate of the PS of x from \mathbf{x} is directly related to the PS of the continuous space-time signal $x(\mathbf{r}, t)$ through a convolution with a kernel. This kernel depends on the location of the space-time samples and on the particular PS estimation method used. In the case of the MVE, the kernel is translation-variant. The fact that the PS of x estimated from \mathbf{x} is the convolution of the PS of x with a kernel provides the formal link between the clutter PS locus described in the previous section and the estimate of the clutter PS obtained from sampled data. This is illustrated in Fig. 4 where the convolution kernel corresponding to the MVE and a 12 elements circular antenna is shown together with the corre-

²The 4D clutter PS locus is actually depicted as a projection in the 3D (v_d, v_{sa}, v_{sc}) -space.

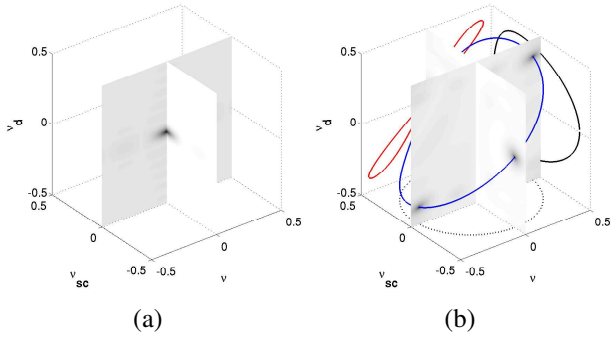


Figure 4: (a) Convolution kernel (in grayscale) linking the MVE PS based on \mathbf{x} and the PS of x . (b) Comparison between the clutter PS (grayscale) and the clutter PS locus (blue line) for a 12 elements circular antenna.

sponding clutter PS. As can be seen, the clutter PS is indeed concentrated along the clutter PS locus. Similarly, Fig. 5 shows the convolution kernel and the clutter PS in the case

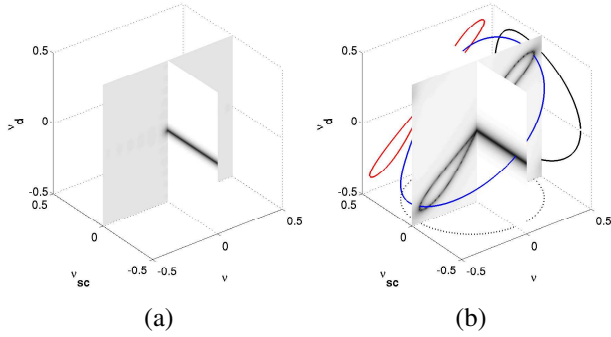


Figure 5: (a) Convolution kernel (in grayscale) linking the MVE PS based on \mathbf{x} and the PS of x . (b) Comparison between the clutter PS (grayscale) and the clutter PS locus (blue line) for a 12 elements ULA.

of a ULA. As was to be expected, in the latter case the clutter PS does not depend on the cross-track and vertical spatial-frequency components. It only varies with k_x and ω .

3. RANGE-DEPENDENCE OF THE CLUTTER POWER SPECTRUM

For monostatic scenarios and for most bistatic scenarios, the 4D clutter PS locus will depend on the range considered. Figure 6 illustrates this for a bistatic scenario and Fig. 7 for a monostatic scenario. For monostatic scenarios, the 4D clutter PS locus resides on a 3D hyperplane. The consequence is that the projection of the clutter PS locus on a suitably oriented 2D plane yields overlapping straight lines at any range. This happens when the considered 2D plane

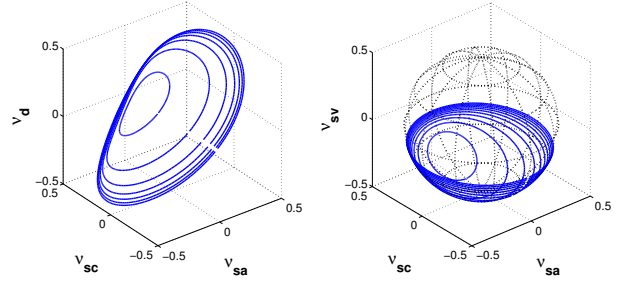


Figure 6: Evolution of the 4D clutter PS locus for increasing range in the case of a wing-to-wing bistatic scenario.

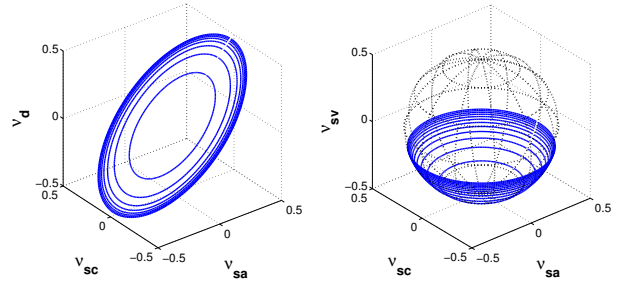


Figure 7: Evolution of the 4D clutter PS locus for increasing range in the case of a monostatic scenario.

is oriented parallel to the platform velocity vector. This indeed means that the linear antenna must be parallel to the velocity vector.

The conditions under which the 2D PS locus is independent of the range are derived in [16] in the case of an ULA, a uniform PRI, and a horizontal velocity. This derivation is based on an explicit expression of the equations of the 2D clutter PS locus. From the 4D clutter PS locus, we can arrive at the same conclusions by a simple argument. First, we consider the spatial frequencies. For the clutter PS locus to be independent of range, the curves at different ranges need to overlap in the 3D space of the spatial frequencies. Since the elevation of points along the curves in the 3D space of the spatial frequencies only depends on the elevation angle at which the scatterers along the isoranges are seen from the receiver, overlap in the 3D space of the spatial frequencies occurs if and only if the receiver is on the (flat) ground. In this case, the scatterers are seen at an elevation angle of zero regardless of range. Second, we consider the Doppler frequency. We require that the Doppler frequency corresponding to a particular spatial frequency be independent of range. In a configuration where the receiver is located on the ground, the Doppler frequency shift due to the receiver velocity will be constant along radial lines from the receiver. The only configurations for which the Doppler frequency shift induced by the transmitter velocity is independent of range is either

- when the transmitter is static (including no vertical velocity component), in which case this Doppler frequency is zero and hence independent of range, or
- when the transmitter is located on the ground and at the same location as the receiver, in which case the Doppler frequency only depends on the transmitter azimuth angle (and on the transmitter velocity) which is independent of range. Notice that in this case, the velocity of the transmitter may be different from that of the receiver.

In the case where the 4D clutter PS locus depends on range, an estimate of the clutter CM using the sample CM will be biased since the averaged snapshots will not be identically distributed. This is illustrated in the case of a 12-elements circular antenna in Fig. 8, where the clutter PS estimated from the sample CM is presented. As can be seen,

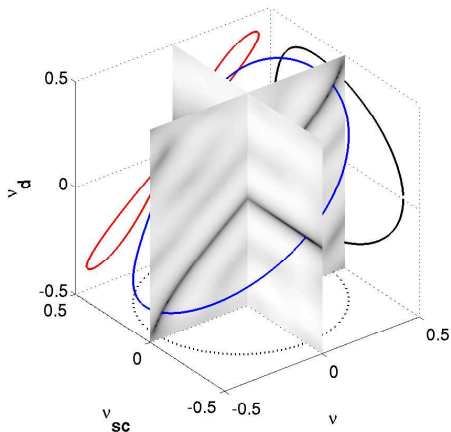


Figure 8: MVE clutter PS estimated from the sample CM.

the PS significantly deviates from the true clutter PS estimate based on the clairvoyant CM depicted in Fig. 4.

4. RANGE-DEPENDENCE COMPENSATION

The registration-based range-dependence compensation method (RBC) described in [1, 2] and developed for a ULA will now be generalized to arbitrary antenna arrays. The original method relies on the registration of the 2D clutter PS locus at the different ranges and consists of three steps:

1. An analysis step, where the 2D PS of the snapshot at each range is independently computed along the 2D clutter PS locus at the corresponding range.
2. A registration step, where the 2D PS at different ranges are averaged along so-called flow lines.

3. A synthesis step where the covariance matrix at the range of interest is synthesized from the 2D PS along the 2D clutter PS locus at the range of interest.

Given the discussion of the 4D clutter PS locus in Sections 2 and 3, the generalization consists (a) in performing the analysis along the 4D clutter PS locus at each range and (b) in performing the synthesis along the 4D clutter PS locus at the range of interest. This generalization allows one to apply this method to any antenna array and any scenario, including that of the monostatic ULA. Figure 9 shows the clutter PS estimated using this method in a bistatic scenario with a 12 element circular array.

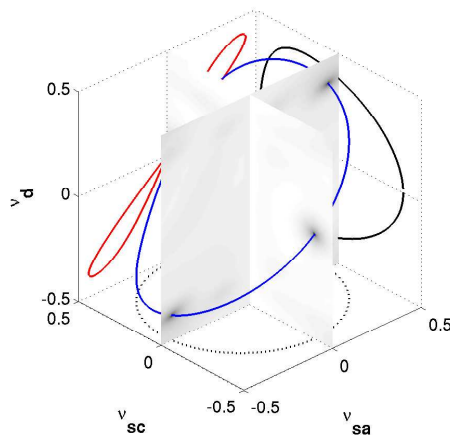


Figure 9: MVE clutter PS from the CM estimated using the proposed method.

5. RESULTS

The quality of the estimated interference+noise covariance matrices can be measured by the SINR loss [3]. Figure 10 shows the SINR loss obtained using the proposed method (RBC). For comparison, the performance of the optimum processor (OP) and that of the sample matrix inversion (SMI) are also shown. The training set for the RBC and SMI methods contained 129 snapshots. The performance of the proposed methods is very close to that of the OP. Due to the range-dependence of the clutter PS, the SMI causes overnulling (signal cancellation).

6. CONCLUSIONS

The concept of correlations and PS in STAP were generalized from 2D (linear antenna) to 4D (non-linear antenna). We show that the 2D PS is the projection of the 4D PS. This is a direct consequence of the projection-slice theorem well known in computerized tomography. The same projection

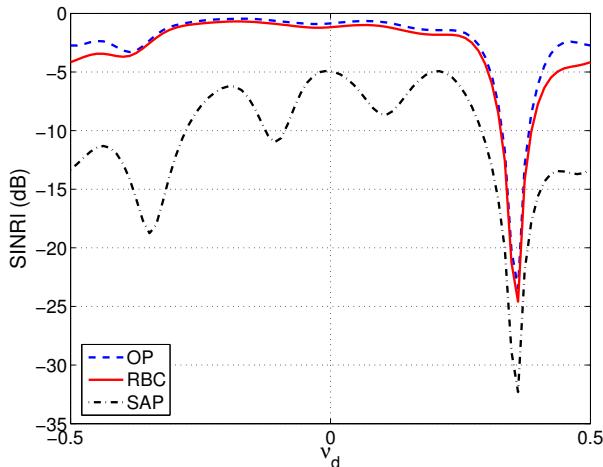


Figure 10: Comparison of the SINR loss of the registration-based compensation (RBC) method with that obtained using the optimum processor (OP) and the sample matrix inversion (SMI) method.

property holds between the 2D clutter PS locus and the 4D clutter PS locus. This property provided insight into the behavior of the 2D clutter PS locus. In particular the effect of crab angle can be modeled as a rotation in the 4D spectral domain.

The registration-based range-dependence compensation method of [1, 2] was generalized to non-linear arrays using the 4D clutter PS locus. Finally, the performance of the proposed range-dependence compensation method was evaluated in terms of SINR loss and found to be very close to that of the optimum processor.

7. REFERENCES

- [1] F. D. Lapierre and J. G. Verly, "Registration-based solutions to the range-dependence problem in STAP radars," in *Adaptive Sensor Array Processing (ASAP) Workshop*, MIT Lincoln Laboratory, Lexington, MA, Mar. 2003.
- [2] F. D. Lapierre, Ph. Ries, and J. G. Verly, "Computationally-efficient range-dependence compensation methods for bistatic radar STAP," in *Proceedings of the IEEE Radar Conference 2005*, Arlington, VA, May 2005.
- [3] J. Ward, "Space-time adaptive processing for airborne radar," Tech. Rep. 1015, MIT Lincoln Laboratory, Lexington, MA, Dec. 1994.
- [4] Richard Klemm, *Principles of space-time adaptive processing*, The Institution of Electrical Engineers (IEE), UK, 2002.
- [5] Y. Zhang and B. Himed, "Effects of geometry on clutter characteristics of bistatic radars," in *Proceedings of the IEEE Radar Conference 2003*, Huntsville, AL, May 2003.
- [6] Michael Zatman, "Circular array STAP," *IEEE Transactions on Aerospace and Electronic Systems*, vol. 36, no. 2, pp. 510–517, Apr. 2000.
- [7] Hien N. Nguyen, John D. Hiemstra, and J. Scott Goldstein, "The reduced rank multistage Wiener filter for circular array STAP," in *Proceedings of the IEEE Radar Conference 2003*, Huntsville, AL, May 2003.
- [8] K. Kim, T. K. Sarkar, and M. S. Palma, "Adaptive processing using a single snapshot for a nonuniformly spaced array in the presence of mutual coupling and near-field scatterers," *IEEE Transactions on Antennas and Propagation*, vol. 50, no. 5, pp. 582–590, May 2002.
- [9] R. K. Hersey, W. L. Melvin, and J. H. McClellan, "Clutter-limited detection performance of multi-channel conformal arrays," *Signal Processing*, vol. 84, pp. 1481–1500, May 2004.
- [10] K. Kim, Y. Zhang, A. Hajjari, and B. Himed, "A uniform planar virtual array approach to conformal array STAP," in *Proceedings of the Int. Radar conference 2004*, Toulouse, FR, Oct. 2004.
- [11] Harry L. Van Trees, *Optimum Array Processing*, Wiley, 2002.
- [12] J. Capon, "High-resolution frequency-wavenumber spectrum analysis," *Proceedings of the IEEE*, vol. 57, no. 8, pp. 1408–1419, Aug. 1969.
- [13] Robert M. Gray and Joseph W. Goodman, *Fourier Transforms: An Introduction for Engineers*, Kluwer Academic Publishers, 1995.
- [14] X. Neyt, F. D. Lapierre, and J. G. Verly, "Principle and evaluation of a registration-based range-dependence compensation method for STAP in case of arbitrary antenna patterns and simulated snapshots," in *Proc. Adaptive Sensor Array Processing Workshop*, MIT Lincoln Laboratory, Lexington, MA, Mar. 2004.
- [15] W. L. Melvin, M. J. Callahan, and M. E. Davis, "Comparison of bistatic clutter mitigation algorithms for varying geometries," in *Proceedings of the IEEE Radar Conference 2005*, Arlington, VA, May 2005.
- [16] F. D. Lapierre, *Registration-based Range-dependence Compensation in Airborne Bistatic Radar STAP*, Ph.D. thesis, University of Liège, Nov. 2004.